Chemistry & Biology
Article

Glycosidase Inhibition by Macrolide Antibiotics Elucidated by STD-NMR Spectroscopy

Ali Sadeghi-Khomami,[1,2] Michael D. Lumsden,[2] and David L. Jakeman[1,2,*]
[1]College of Pharmacy
[2]Department of Chemistry
Dalhousie University, Halifax, NS, B3H 1E9, Canada
*Correspondence: david.jakeman@dal.ca
DOI 10.1016/j.chembiol.2008.05.017

SUMMARY

A glycosynthase approach was attempted to glycodiversify macrolide antibiotics, using DesR, a family-3 retaining β-glucosidase involved in the self-resistance mechanism of methymycin production. STD-NMR was used to probe enzyme-substrate interactions. Analysis of competitive STD-NMR experiments between erythromycin A and a chromogenic substrate (*p*NP-β-D-glucose) with the hydrolytically inactive nucleophile mutants led us to discover a family of unprecedented glycosidase inhibitors. Analysis of kinetic data with wild-type DesR determined that erythromycin is a competitive inhibitor of the glucosidase (IC_{50} = 2.8 ± 0.3 μM and K_i = 2 ± 0.2 μM) with respect to the hydrolysis of *p*NP-β-D-glucose. Comparable inhibitory data was obtained for clarithromycin; however, the inhibitory effect of azithromycin was weak and no significant inhibition was observed with methymycin or D-desosamine. This report documents significant inhibition of glycosidases by macrolide antibiotics and provides insight into the design of novel glycosidase inhibitors based on the macrolactone ring of macrolide antibiotics.

INTRODUCTION

Macrolide antibiotics have broad bacteriostatic action against many Gram-positive bacteria and function by binding to the ribosome (Sweetman, 2002; Schlunzen et al., 2001). Recently they have also been considered for nonantimicrobial applications such as gastrointestinal stimulating (Omura et al., 1985; Armstrong et al., 1992; Erbas et al., 1993; Hawkyard and Koerner, 2007), immunomudulatory (Giamarellos-Bourboulis, 2008; Rubin, 2004), anti-inflammatory (Zalewska-Kaszubska and Gorska, 2001; Culic et al., 2001; White and Simon, 2005; Ianaro et al., 2000), antitumor (Yatsunami et al., 1999; Wang et al., 2000), and anti-HIV (San Jose et al., 1997) activities. There are several ongoing structure-activity relationship and mechanism of action studies to differentiate these broad ranges of activities. Macrolide antibiotics (e.g., methymycin, erythromycin, clarithromycin, azithromycin) are composed, in part, of carbohydrate functionalities (Figures 1A and 1B) that play important roles in binding, efficacy, potency, and resistance (Thibodeaux et al., 2007; Thibodeaux and Liu, 2007; Zhang et al., 2007; Walsh et al., 2003). Thus, the modification of the carbohydrate functionalities is an important approach for drug development and discovery (Fu et al., 2003; Mendez and Salas, 2001; Thibodeaux et al., 2007; Thibodeaux and Liu, 2007; Yang et al., 2004; Griffith et al., 2005), particularly in view of the prevalence of bacterial resistance toward many antibacterial drugs (Henninger, 2003; Coates et al., 2002).

Current strategies for in vitro glycosylation of natural products are multistep chemical synthesis, enzymatic glycosylation using glycosyltransferases and costly sugar-nucleotide substrates, or reversible glycosidases (Thiem, 1995). To overcome these limitations, glycosynthase enzymes were engineered from glycosidases via replacement of the nucleophilic carboxylate (Asp or Glu) to Ala, Ser, or Gly (Jakeman and Withers, 2002). Thus, in the presence of suitable glycosyl donors, mimicking the glycosyl-enzyme adduct, e.g., α-glycosyl fluorides, glycosynthase mutants catalyze the formation of a new glycosidic linkage, without any hydrolytic activity (see Scheme S1 available online).

Glycosynthases have primarily arisen from endo- or exo-retaining β-glycosidases (Hancock et al., 2006) that physiologically cleave oligo- or polysaccharides, although recently glycosynthase approaches toward glycosphingolipids (Vaughan et al., 2006), glycosylated flavonoids (Yang et al., 2007), and an inverting glycosidase (Honda and Kitaoka, 2006) have been described. There is no report on glycosylation of macrolide antibiotics using these catalysts. We identified DesR, a family-3 β-(1-2)-glucosidase (EC # 3.2.1.21) from *Streptomyces venezuelae* involved in the self-resistance mechanism for methymycin biosynthesis (Figure 1B) (Zhao et al., 1998, 2003), as a potential glycosynthase that would potentially catalyze the formation of a β-(1-2) glycosidic linkage.

It has been known that not all glycosidase nucleophile mutants function as glycosynthases (Ducros et al., 2003), thus different techniques have been applied to investigate the efficiency of these mutants including fluoride-releasing activity (Drone et al., 2005), external nucleophile rescue experiments (Hommalai et al., 2007), circular dichroism (Salleh et al., 2006), and X-ray crystallography analysis (Jahn et al., 2003; Pyetan et al., 2007). Saturation transfer difference nuclear magnetic spectroscopy (STD-NMR) is a powerful technique that could be used in

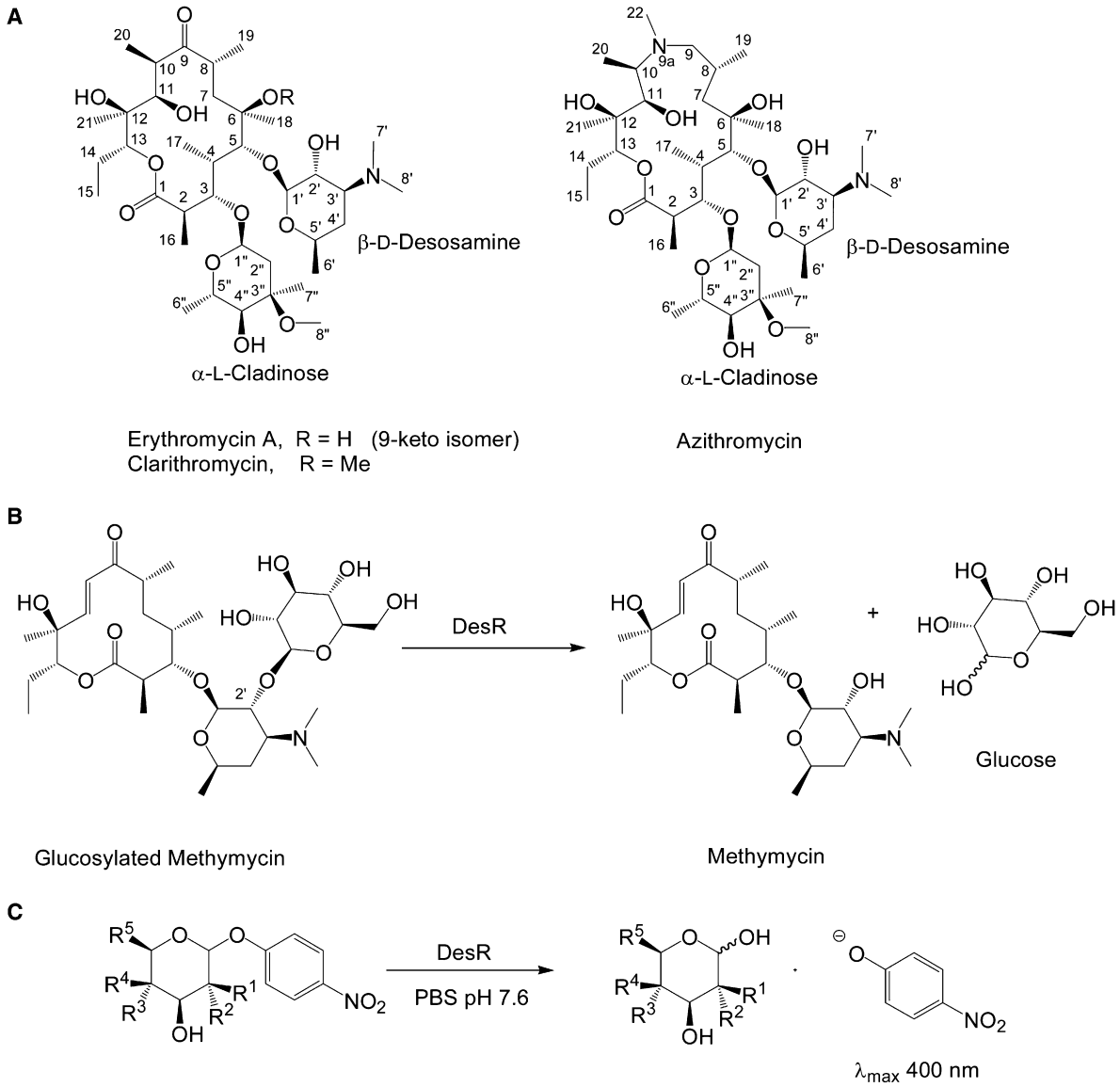

Figure 1. Structures of Macrolides and the Role of Glucosidase Self-Resistance

(A) Structure of macrolide antibiotics. Reactions catalyzed by DesR-WT.

(B) Production of methymycin from glucosylated precursor.

(C) Release of *para*-nitrophenolate from a series of *p*NP-glycosides was measured based upon absorbance at 400 nm (see Figure 2 for structural and kinetic information).

solution for characterization of ligand binding at atomic resolution; however, it has only rarely been applied to glycosidases (Wen et al., 2005; Berteau et al., 2003; Haselhorst et al., 2004; Brecker et al., 2006).

Here we report our attempts toward development of potential glycosynthases for macrolide antibiotic acceptors from DesR, and we will describe application of STD-NMR spectroscopy in analysis of ligand binding with catalytically inactive glycosidase nucleophile mutants. Our results indicate a new application for STD-NMR studies in discovery of novel glycosidase inhibitory effect of macrolide antibiotics.

RESULTS

Analysis of 3D structures of two members of family-3 glycosidases (β-N-acetylhexosaminidase [Williams et al., 2002] and exo-1,3-1,4-glucanase [Hrmova and Fincher, 2001]) and an amino acid sequence alignment showed that aspartic acid 273 of DesR was the conserved amino acid and it may play the role of nucleophile in catalysis (Figure S1). Recombinant DesR-WT and DesR-D273G, DesR-D273A, DesR-D273S mutants were prepared by site-directed mutagenesis. They were expressed using *E. coli* in soluble form at high levels (ca. 100 mg l^{-1} of

culture) and were purified to >95% purity (Figure S2). No significant differences in yields were noticed between the expression of DesR-WT and any of the mutants. The BugBuster reagent and protein expression at 20°C were essential for preparation of soluble DesR.

A small library of commercially available *p*NP-glycosides was screened against the purified enzymes, and it was discovered that *p*NP-β-D-Glc was accepted as a chromogenic substrate for DesR-WT (Figures 1C, 2A, and 2B). No other *p*NP-glycosides were sufficiently active to enable the determination of kinetic parameters, although low levels of hydrolytic activity were observed with *p*NP-α-D-Glc. The optimum pH activity for hydrolysis of *p*NP-β-D-Glc was determined to be bell-shaped, centered between pH 7.5 and pH 8.5 (Figures 2C and S3), which is indicative of two ionizable functionalities within the active site (Scheme S1). The rate of hydrolysis of *p*NP-β-D-Glc allowed us to calculate the following kinetic parameters: K_m 4.7 ± 0.5 mM, V_{max} 19.1 ± 1 μmol min^{-1} mg^{-1} (Figure 2B). The DesR-WT specific activity was 2 U mg^{-1} for hydrolysis of *p*NP-β-D-Glc and the enzyme was active for several months at 4°C. The enzyme could tolerate multiple freeze/thaw cycles, up to 10% (vol) ethanol, 500 mM phosphate, and raising assay temperatures to 35°C without significant loss of activity. Time-dependent ^{1}H-NMR studies confirmed DesR-WT as a retaining β-glucosidase, by monitoring the hydrolysis of *p*NP-β-D-Glc in d-PBS (pH ~7.6). The exclusive appearance of β-glucopyranose (δ_H 4.68, $J_{1,2}$ = 8 Hz) was observed, while the anomeric proton signal of α-glucopyranose (δ_H 5.27, $J_{1,2}$ = 3.6 Hz) appeared in the later spectra (Figure S4).

Analysis of the hydrolytic activity of the mutants using *p*NP-β-D-Glc revealed that the D273G substitution resulted in a loss of activity (0.2 mU mg^{-1}), consistent with data from nucleophile mutants of other glucosidases (Wang et al., 1994), whereas the D273A and D273S had no detectable enzyme activity in our assay conditions. All mutants were also inactive against all other commercial *p*NP-glycosides (Figure 2A). A dramatic loss of hydrolytic activity for the D273 mutants supports the identification of D273 as the nucleophilic amino acid catalyst of DesR. ^{1}H-NMR spectra of the wild-type and mutant enzymes were essentially identical, showing that the mutants were likely properly folded (Figure S5).

The glycosynthase activity of the three DesR mutants was tested. No product was produced after incubation of mutants with GlcF and methymycin or erythromycin (Figure S6). A variety of conditions were explored, such as varying substrate concentrations, incubation times, and temperature or using cosolvents (ethanol, acetonitrile), with no apparent effect on the result. Incorporation of other potential acceptors in the assay, as described in the Experimental Procedures, did not result in any glycosylation activity. The hydrolysis of GlcF in the absence or in the presence of the enzymes was examined by ^{19}F-NMR, to see if water could function as the acceptor (Figure S7). No significant difference was observed in the rate of hydrolysis of GlcF by DesR-WT or DesR-D273G, consistent with other β-(1-3)-glycoside mutants (Drone et al., 2005). In contrast, the folding of the mutants was further corroborated by external nucleophile rescue experiments; formate anions were able to rescue the hydrolytic activity of the serine and glycine mutants with DNP-β-D-Glc and weakly inhibited DesR-WT activity (Figures S8 and S9).

To see whether nonproductive binding configurations of *p*NP-β-D-Glc or misfolding of mutants was the reason for the lack of hydrolytic activity, we probed substrate binding to DesR-WT and mutants using STD-NMR spectroscopy. Recognition of the slow substrate, *p*NP-α-D-Glc, by DesR-WT was determined through the appearance of STD signals (Figure 3A). Comparable binding results were obtained from STD-NMR experiments involving *p*NP-α- and β-D-Glc with the D273S mutant, implying that hydrolytically competent substrates were also recognized by the mutant (Figures 3B–3D and S12). An STD-NMR spectrum from an equimolar mixture of *p*NP-α- and β-D-Glc interacting with the D273S mutant indicated that both aryl glycosides bound (Figure 3D), particularly given the presence of signals from H1 and the ortho substituents of the phenyl rings. The binding of *p*NP-α-D-Glc to the wild-type enzyme and D273S mutant was observed by STD-NMR with comparable intensity; however, there were subtle differences between the STD-enhancements observed (Figure S13). In particular, H1 and H5 intensities were both 23% with the wild-type enzyme, whereas H1 and H5 intensities were both 80% with the D273S mutant.

STD-NMR spectroscopy was applied to probe whether the fluorosugar and macrolide substrates bound to the mutant enzyme. STD-NMR signals were observed for erythromycin and GlcF, indicating that both compounds were recognized by the D273S mutant (Figures 4A and 5B). Also, STD-NMR studies revealed that the interaction between GlcF and the D273S mutant was greater than with DesR-WT (Figures 4A and 4E). When a mixture of GlcF and glucose in the presence of the D273S mutant was analyzed by STD-NMR, only GlcF, not the α or β forms of glucopyranose, bound to the mutant. In the unlikely event that either glucopyranose form bound as a high-affinity ligand with a slow k_{off} rate (Wang et al., 2004), competition-binding experiments were performed by titration of glucose into the mixture of GlcF and D273S mutant (Figures 4B–4D). Signals were not observed for either glucopyranose form binding to D273S.

The wild-type enzyme and nucleophile mutant both bound erythromycin based on STD-NMR results (Figures 5A and 5B). In an attempt to demonstrate a partially overlapping binding site for erythromycin and *p*NP-β-D-Glc, and to rule out nonspecific interactions, a competitive STD-NMR titration experiment was performed in which erythromycin was added to a mixture of *p*NP-β-D-Glc and the D273S mutant (Figures 5C–5E). However, the solubility of erythromycin limited the titration. The STD-NMR signal intensity of *p*NP-β-D-Glc decreased after addition of erythromycin, indicating that the antibiotic likely competes with *p*NP-β-D-Glc in an overlapping binding site. We fully assigned the ^{1}H NMR spectrum of erythromycin in d-PBS (pH ~7.6) at 27°C to determine the binding-epitope of erythromycin using STD-NMR spectroscopy (Tables S2 and S3). A confounding factor is the existence of the hemiacetal forms of erythromycin (Barber et al., 1991). It was determined that the concentration of the 9,12-hemiacetal isomer of erythromycin was 2.3 times less than the 9-keto isomer (Figure S16). We determined that D-desosamine and L-cladinose were found in $^4C_1$ and $^1C_4$ conformations, respectively. We did not observe a significant STD enhancement with the 9,12-hemiacetal form of erythromycin in 1D ^{1}H-STD-NMR experiments (Figure 6B). Group epitope mapping of erythromycin bound with DesR-D273S mutant (Figure 6C) was determined using 2D STD-TOCSY NMR (Figure S15) and revealed that

A

Entry	Compound	R^1	R^2	R^3	R^4	R^5	K_m μM	V_{max} μmol min^{-1} mg^{-1}	V_{max} / K_m x10^3
1	*p*NP-β-D-Glc	H	OH	OH	H	CH_2OH	4713±500	19.1±1	4.05
2	*p*NP-α-D-Glc	H	OH	OH	H	CH_2OH	-*	-*	-*
3	*p*NP-β-D-Xyl	H	OH	OH	H	H	-	-	-
4	*p*NP-β-D-Glu	H	OH	OH	H	CO_2H	-	-	-
5	*p*NP-β-D-GlcNAc	H	$NHCOCH_3$	OH	H	CH_2OH	-	-	-
6	*p*NP-β-D-Gal	H	OH	H	OH	CH_2OH	-	-	-
7	*p*NP-α-D-Gal	H	OH	H	OH	CH_2OH	-	-	-
8	*p*NP-β-D-Fuc	H	OH	H	OH	CH_3	-	-	-
9	*p*NP-β-D-Man	OH	H	OH	H	CH_2OH	-	-	-
10	Methymycin-β-D-Glc†	H	OH	OH	H	CH_2OH	4.1±0.1	0.585±0.004	142.7

- no activity * very weak unquantifiable activity was observed † (Zhao et al., 2003)

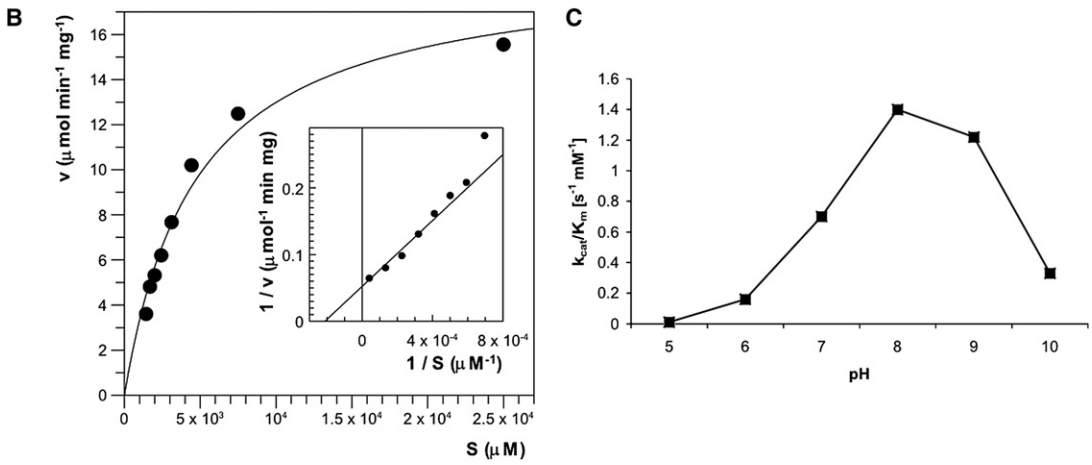

Figure 2. Kinetic Analysis of Wild-Type DesR

(A) Screening of chromogenic substrates with DesR-WT.

(B) Representative kinetic data for the reaction of DesR-WT with *p*NP-β-D-Glc (K_m 4.7 ± 0.5 mM, k_{cat} 19.1 ± 1 μmol min^{-1} mg^{-1}). The assays were performed as described in the Experimental Procedures using 0.5 μM enzyme. Time-dependent changes were monitored at 400 nm and initial rates were used for kinetic calculations. Each point was measured in triplicate. (Outer graph) Michaelis-Menten plot: the lines through the points represent the Michaelis-Menten equation calculated by the GraFit. (Inset) Lineweaver-Burk plot.

(C) pH dependence of the hydrolysis of *p*NP-β-D-Glc by DesR-WT; the line was added to data points for better visualization.

D-desosamine and L-cladinose sugars, as well as the macrolactone ring, were involved in interactions with the enzyme.

Inhibition studies indicated that erythromycin was a potent β-glucosidase inhibitor (IC_{50} = 2.8 ± 0.3 μM) (Figure 7A). Detailed kinetic analysis determined that erythromycin was a competitive inhibitor of DesR-WT, with a K_i = 2 ± 0.2 μM (Figures 7B and 7C). Two semisynthetic macrolides, clarythromycin and azithromycin, which are more acid stable and exist as a single isomer in aqueous solution (Awan et al., 1992; Fiese and Steffen, 1990), were examined as glycosidase inhibitors. Clarythromycin, a 14 membered macrolide, was also found to be a competitive inhibitor for DesR-WT (IC_{50} 9.7 ± 0.6 μM [Figure 7]; K_i = 6.2 ± 1.2 μM, K_i, [data not shown]), whereas azithromycin, a 15 membered macrolide antibiotic that has the sugars in the same conformations and orientations as in the erythromycin derivatives (Lazarevski et al., 1993), recorded an IC_{50} of 459 ± 88 μM (Figure 7A). Additionally, no significant inhibition of DesR was observed when the physiological product of the enzyme, methymycin, or D-desosamine, was examined up to a final concentration of 400 μM and 250 mM, respectively.

DISCUSSION

We identified DesR, a β-(1-2) glucosidase, as a potential glycosynthase enzyme that would generate novel macrolide

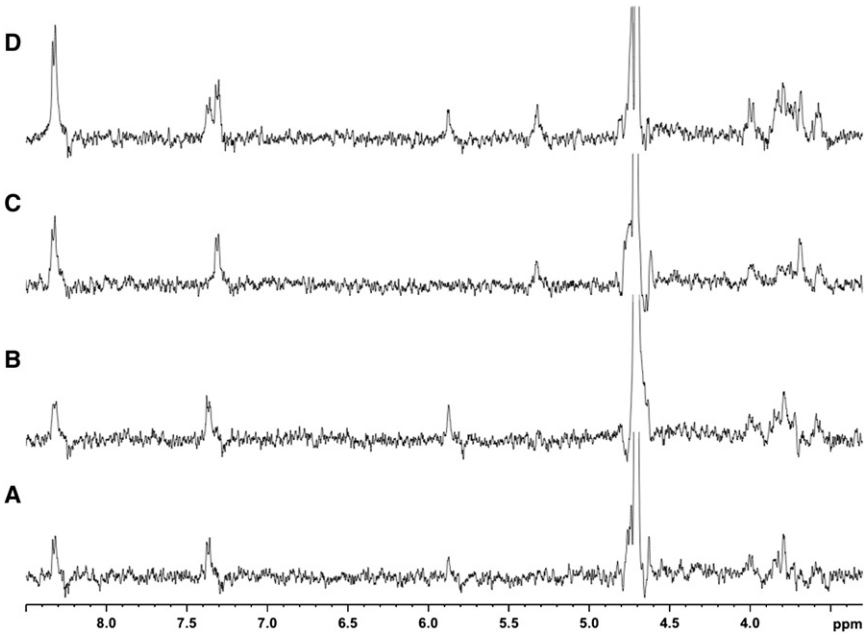

Figure 3. STD-NMR Spectra of *p*NP-α- and *p*NP-D-Glc Binding to DesR Wild-Type and to Hydrolytically Inactive Mutant D273S

500 MHz ^{1}H-STD-NMR spectrum in d-PBS (pH ~7.6): (A) DesR-WT (0.02 mM) and *p*NP-α-D-Glc (2 mM); (B) DesR-D273S (0.02 mM) and *p*NP-α-D-Glc (2 mM); (C) DesR-D273S (0.02 mM) and *p*NP-β-D-Glc (2 mM); (D) DesR-D273S (0.02 mM), *p*NP-β-D-Glc (2 mM), and *p*NP-α-D-Glc (2 mM).

antibiotics. In addition, glycosynthases have not been developed that catalyze the formation of β-(1-2) linkages or linkages to amino sugars. Following the expression and purification of DesR-WT, we found that *p*NP-β-D-Glc was a substrate for DesR-WT, in contrast to its homolog, OleR (Quiros et al., 1994). Further analysis of DesR-WT catalysis confirmed the enzyme was a β-retaining glucosidase with similar pH activity profiles for *p*NP-β-D-Glc and the physiological substrate (Zhao et al., 2003). The K_m for the physiological substrate indicated a 1000-fold tighter binding affinity than the aryl glucoside, while the physiological substrate has a 30-fold lower V_{max}. Overall, this results in a 35-fold reduction of V_{max}/K_m for the aryl glucoside (Figure 2A). To the extent that K_m is a measure of substrate binding, these results indicate that there is most likely a significant interaction between DesR-WT and the macrolactone ring in the acceptor binding site. This implies an extended acceptor-binding site on DesR, since it would be anticipated that the macrolactone binds a substantial distance from the active site catalytic residues. The 30-fold higher V_{max} for the aryl glucoside is likely a result of the substantial decrease in pK_{HA} of the *p*-nitrophenolate relative to the secondary alcohol. A dramatic loss of hydrolytic activity for the D273 mutants supports the identification of D273 as the nucleophilic amino acid catalyst of DesR. Further support is given through the rescue experiments with the nucleophile mutants, where the cleavage of DNP-β-D-Glc with formate indicated that the mutants were also properly folded. Moreover, the STD-NMR experiments demonstrated that erythromycin (Figures 5A and 5B) and *p*NP-α-D-Glc (Figures 3A and 3B) were recognized by the mutants and the wild-type enzyme similarly; reconfirming the proper folding of the mutants. Therefore, the lack of hydrolytic activity with the mutants was likely due to a change of the catalytic machinery.

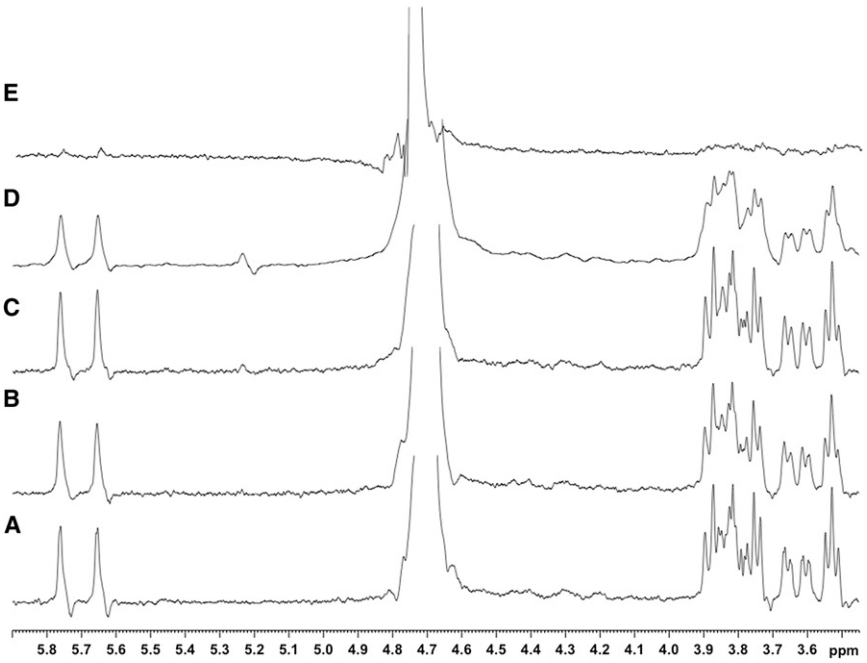

Figure 4. STD-NMR Spectra of GlcF Binding to DesR Wild-Type and to Hydrolytically Inactive Mutant D273S

500 MHz ^{1}H-STD-NMR spectrum of DesR-D273S (0.1 mM) in d-PBS (pH ~7.6) in the presence of (A) GlcF (20 mM), (B) A + D-Glc (1 mM), (C) A + D-Glc (2 mM), (D) A + D-Glc (20 mM), and (E) 500 MHz ^{1}H-STD-NMR spectrum of DesR-WT (0.1 mM) and a mixture of GlcF: α-D-Glc: β-D-Glc (5.2:1:1.5) in d-PBS (pH ~7.6).

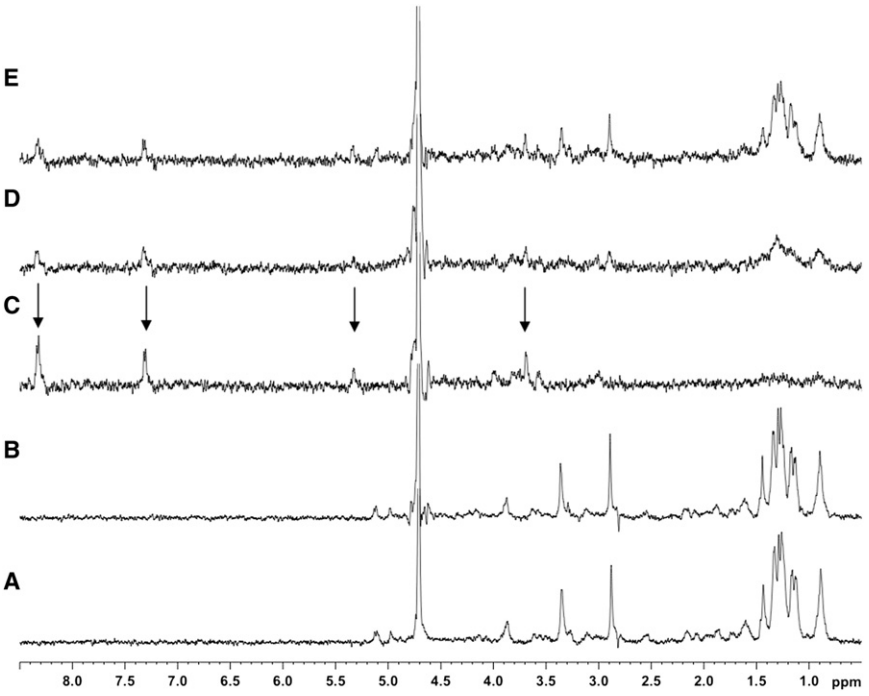

Figure 5. STD-NMR Spectra of Erythromycin and *p*NP-β-D-Glc Binding to Hydrolytically Inactive Mutant D273S

500 MHz ^{1}H-STD-NMR spectrum in d-PBS (pH ~7.6): (A) DesR-WT (0.02 mM) and erythromycin (2 mM), (B) DesR-D273S (0.02 mM) and erythromycin (2 mM), (C) DesR-D273S (0.02 mM) and *p*NP-β-D-Glc (2 mM), (D) C + erythromycin (0.1 mM), and (E) C + erythromycin (0.32 mM). NMR signals in *p*NP-β-D-Glc that were noticeably suppressed upon addition of erythromycin are marked by arrows.

Our STD-NMR experiments demonstrated that the nucleophile mutants bound GlcF (Figure 4A) and erythromycin (Figure 5B), despite being catalytically inactive in transglycosylation mode. It also revealed that GlcF binds to the mutants better than the WT enzyme, supporting the hypothesis that glycosidase nucleophile mutants more efficiently bind GlcF. The incorporation of an α-fluoro substituent at C1 of glucose is essential for recognition and binding by the nucleophile mutants, since neither the α or β forms of glucose bind (Figure 4E).

Our STD-NMR data indicate that *p*NP-α-D-Glc binds to the wild-type and the D273S mutant with comparable intensity. In both instances, signals corresponding to the carbohydrate and the aryl moiety were clearly observed. There were changes in STD signal intensities, relative to the largest intensities in each difference spectrum, for particular protons in *p*NP-α-D-Glc. The H1 and H5 intensities were both 23% with the wild-type enzyme, whereas H1 and H5 intensities were both 80% with the D273S mutant. The intensities for the other glucoside protons (H2–4, H6) interacting with the wild type and mutant were similar. Thus, the glucoside binds to both the wild type and D273S mutant, with more intense interactions occurring between the mutant and both H1 and H5 than with the

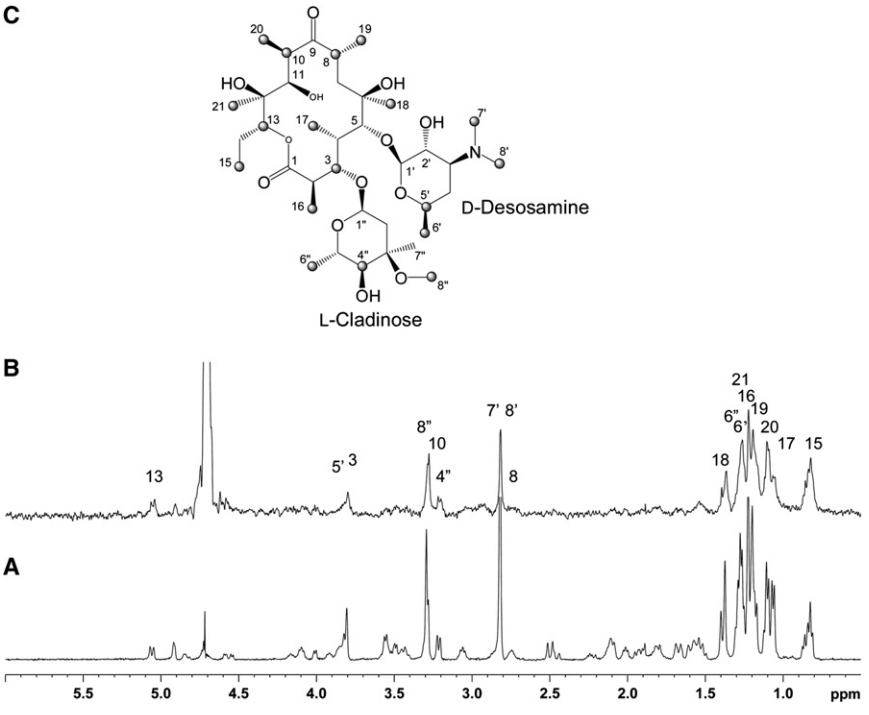

Figure 6. Epitope Mapping of Erythromycin Bound to Hydrolytically Inactive Mutant D273S

(A) 500 MHz ^{1}H-NMR spectrum of erythromycin in d-PBS (pH ~7.6); (B) 500 MHz ^{1}H-STD-NMR spectrum of DesR-D273S (0.1 mM) and erythromycin (2 mM) in d-PBS (pH ~7.6), saturation time 5 s; (C) Epitope mapping of erythromycin A bound to DesR-D273S in d-PBS (pH ~7.6) using 2D STD-TOCSY NMR data. Shaded circles indicate definitive STD enhancement between erythromycin and DesR-D273S.

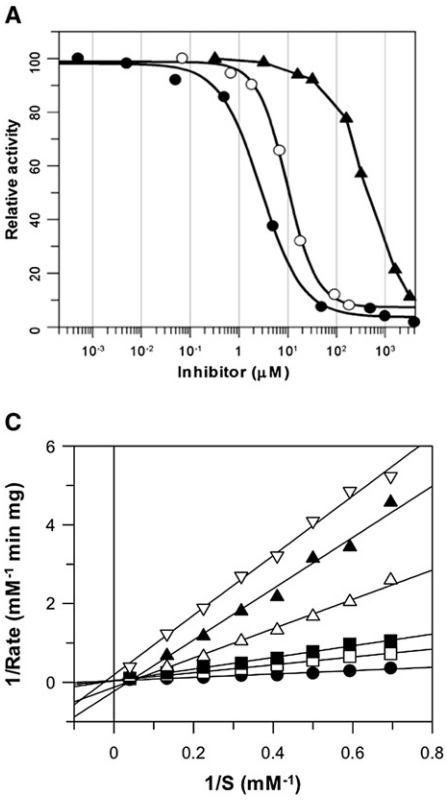

Figure 7. Inhibition of DesR Wild-Type by Erythromycin and Related Macrolide Antibiotics

(A) Representative IC_{50} data for the inhibition of *p*NP-β-D-Glc hydrolysis by DesR-WT with ● erythromycin (IC_{50} = 2.8 ± 0.3 μM), ○ clarithromycin (IC_{50} = 9.7 ± 0.6 μM), and ▲ azithromycin (IC_{50} = 459 ± 88 μM).

(B and C) Michaelis-Menten plot (B); Lineweaver-Burk plot (C) (1 mM data have not been shown for clarity purposes), lines drawn obtained from nonlinear least-squares fit to the observed data using Michaelis-Menten equation for competitive inhibition of erythromycin (K_i = 2.0 ± 0.2 μM).

Inhibition of *p*NP-β-D-Glc hydrolysis by DesR-WT (○, no erythromycin; ●, 0.001; ▽, 0.005; ■, 0.01; △, 0.1; ▲, 0.2; □, 0.5; and ▼, 1 mM). The final concentration of enzyme was 0.5 μM and concentrations of *p*NP-β-D-Glc (S) were between 1.4 and 25 mM.

wild-type enzyme and these protons. The STD-NMR data for the D273S mutant indicated that *p*NP-β-D-Glc and *p*NP-α-D-Glc bind with comparable intensity; analysis of the wild-type enzyme with *p*NP-β-D-Glc was not attempted due to the rapid hydrolysis of this substrate.

Erythromycin bound to both the wild-type enzyme and the D273S mutant with essentially identical STD-NMR spectra. The interpretation of our STD-NMR data for erythromycin did not include accounting for the effects of differential relaxation times of each proton, which has been shown to have an effect upon quantitative epitope mapping (Yan et al., 2003), due to the significantly crowded nature of the erythromycin ^{1}H-NMR spectrum. Thus, the relatively high intensity of the signals arising from the methyl substituents of erythromycin is not necessarily proportional to the strength of the interaction (Berteau et al., 2003). However, the signals clearly identified through analysis of the STD-NMR experiments demonstrated that both sugar rings and the macrolactone ring of erythromycin were involved in interactions with DesR (Figure 6). It is of significance that the L-cladinose residue interacts with DesR, given that it is not a component of methymycin, the physiological substrate. Although recognition of the D-desosamine ring was clear, the lack of an apparent interaction between the C-2′ proton of the D-desosamine ring and DesR may indicate that the desosamine ring binds in an incorrect orientation for transglycosylation with GlcF, given that there is an unequivocal signal for the interaction between C-1 of GlcF and the mutant. Competitive STD-NMR binding experiments between erythromycin and *p*NP-β-D-Glc with DesR-D273S led to a reduction in the binding of *p*NP-β-D-Glc upon addition of erythromycin (Figures 5C–5E), lending support to a hypothesis that these two compounds share an overlapping binding site.

The interactions observed by STD-NMR spectroscopy were substantiated by kinetic analysis. Erythromycin was determined to be a competitive inhibitor of DesR-WT in the hydrolysis of *p*NP-β-D-Glc (IC_{50} = 2.8 ± 0.3 μM, K_i = 2 ± 0.2 μM). The relationship between our IC_{50} and K_i data matches the theoretical relationship closely (Burlingham and Widlanski, 2003). It is significant to note that no glycosidase inhibitory effect was previously observed for erythromycin against *N*-acetyl-β-D-glucosaminidase and lysozyme (Shiono and Hayasaka, 1985). The affinity observed by DesR-WT for erythromycin may potentially explain the lack of glycosynthase activity of the mutants by limiting turnover.

The interaction between the dimethylamino functionality of desosamine and DesR correlates well with the fact that many potent glycosidase inhibitors are aminosugars (Winchester and Fleet, 1992; Dwek et al., 2002) or pseudoaminosugars (Kameda et al., 1985; Takeuchi et al., 1990); thus, we speculated that the desosamine ring of macrolide antibiotics may be responsible for the inhibition of DesR, in an analogous manner to the other 3-aminosugar glycosidase inhibitors (Maxwell et al., 2006). However, no inhibitory effect was observed at high concentrations of desosamine alone. Therefore, we turned our attention to the inhibitory effect of the macrolactone-ring of the antibiotics. We found a dramatic decrease in the inhibition of DesR by azithromycin and methymycin, macrolides of differing ring size to erythromycin. These data support the idea that 14 membered macrolide rings contribute significantly to binding as indicated by STD-NMR and inhibition studies. Based on crystal structure and NMR studies of erythromycin, clarithromycin, and azithromycin, it has been known that the region C(3)–C(8), including the sugars, are almost completely superimposable in 3D structures with variations existing primarily in the conformation of C(9)–C(15) (Awan et al., 1995). Our STD-NMR data (Figure 6), together with glucosidase inhibitory effect of macrolides (Figure 7),

suggest that C(9)–C(15) may play a critical role in inhibition of DesR. This study demonstrates the inhibitory effect of macrolide antibiotics against glycosidases, identifying an alternative class of cyclic natural product glycosidase inhibitors (Rao et al., 2005).

SIGNIFICANCE

STD-NMR spectroscopy enabled us to monitor binding of substrates to inactive enzyme variants, providing insight into the enzyme active site structure and recognition of non-physiological substrates and inhibitors. The spectroscopic investigation explained that substrate binding occurs to glycosidase nucleophile mutants. The lack of glycosynthase activity was likely attributable to a lack of reactivity or binding orientation. Competitive STD-NMR experiments identified that macrolide antibiotics bound to the active site and subsequent kinetic analysis confirmed that the macrolide antibiotics act as competitive glycosidase inhibitors. Whether there is any clinical significance to the inhibition of glycosidases by macrolide antibiotics remains to be determined. The reported inhibition of a glycosidase by a macrolide antibiotic is important because it represents a new chemical scaffold with significant glycosidase inhibition.

EXPERIMENTAL PROCEDURES

Identification of Catalytic Nucleophile Amino Acid

Analysis of 3D structures of two family-3 glycosidase enzymes, a β-N-acetylhexosaminidase (EC # 3.2.1.52) (Williams et al., 2002), and an exo-1,3-1,4-glucanase (EC # 3.2.1.58) (Hrmova and Fincher, 2001) and an amino acid sequence alignment (Clustal W [v 1.83]) between DesR, OleR and EryBI (glucosidases involved in self-resistance of oleandomycin in *Streptomyces antibioticus* (OleR) and erythromycin in *Saccharopolyspora erythraea* (EryBI)) and other homologous glycosidases, showed that aspartic acid 273 was conserved between all proteins (Figure S1).

DesR Mutagenesis

Plasmid pDesR-3 (Zhao et al., 2003) was used as a template for PCR. DesR-D273G, DesR-D273A, and DesR-D273S mutants were prepared with the QuikChange II site-directed mutagenesis kit (Stratagene). Mutagenic primers were synthesized by Integrated DNA Technologies and were designed as follows: 5′-GGC TGG GTG ATG TCC G**G**C T(GG CT**A** GCC) ACC CCG GGC-3′ and 5′-GCC CGG GGT (GGC **T**AG CC)A G**C**C GGA CAT CAC CCA GCC-3′ for mutant D273G; 5′-GGC TGG GTG ATG TCC G**C**C T(GG CT**A** GCC) ACC CCG GGC-3′and 5′-GCC CGG GGT (GGC **T**AG CC)A G**G**C GGA CAT CAC CCA GCC-3′ for mutant D273A; 5′-GC TGG GTG ATG TCC **AGC** T(GG CT**A** GCC) ACC C-3′ and 5′-G GGT (GGC **T**AG CC)A G**CT** GGA CAT CAC CCA GC-3′ for mutant D273S.

A silent mutation was also incorporated into mutagenic primers to create a new restriction site for NheI (bold letter inside the brackets). PCR was performed using a Biometra Tpersonal machine. For PCR, 5 μl each of the pair primers (5 μM) were combined with 3 μl DMSO, 5 μl 10× reaction buffer, 1 μl dNTP mix, 1 μl pDesR-3 (20 ng μl^{-1}) and 29 μl sterile distilled water. After 30 s denaturing at 95°C, 1 μl PfuUltra High-Fidelity DNA-polymerase (2.5 U μl^{-1}) was added and thermocycling was started. The first cycle was 95°C for 30 s (denaturing), 55°C for 1 min (annealing), and 68°C for 7 min (extension), followed by 15 repeating cycles. A DpnI-digested PCR product was transformed into XL1-Blue supercompetent cells. For DesR-D273A and D273S mutants, the QuikChange kit was modified: Pfu DNA polymerase (5 U) (Bio Basic Inc.) was used, the annealing temperature was increased to 65°C, and NovaBlue Giga-Singles competent cells (Novagen) were used for transformations. Transformed cells were grown overnight at 37°C on Luria–Bertani (LB) agar plates including kanamycin (50 μg ml^{-1}). Resistant colonies were individually grown overnight in LB medium supplemented with kanamycin (50 μg ml^{-1}) on a rotary shaker (250 rpm) at 37°C. Plasmid preparations were performed using QIAGEN plasmid purification kits (QIAGEN). Mutants were verified via NheI (NEB) digestion followed by 1% agarose-gel electrophoresis. Finally, mutations were confirmed by sequencing of the mutation point using an up-stream primer (5′-GGC CTC CTT CAT GTG TGC-3′).

Protein Expression

DesR-WT and all engineered DesR mutants were expressed as N-His_6 fusion proteins from pET28b-based expression plasmids in *Escherichia coli* BL21(λDE3) (Novagen). Transformed cells were grown overnight on LB-agar plates including kanamycin (50 μg ml^{-1}). Transformants were grown overnight in LB medium supplemented with kanamycin (50 μg ml^{-1}) on a rotary shaker (250 rpm) at 30°C. Overexpression of proteins was accomplished by transferring a 5 ml inoculum from the overnight culture to 250 ml fresh LB medium containing kanamycin (50 μg ml^{-1}) and grown (30°C) until the optical density at 600 nm (OD_{600}) reached 0.3. Cultures were cooled to 20°C and incubated to mid-log phase (OD_{600} ~0.5). Isopropyl-β-D-thiogalactopyranoside (IPTG) was added to a final concentration of 1 mM to induce protein expression. The cultures were then incubated at 20°C for 20 hr. The cells were collected by centrifugation (4000 × g, 4°C, 60 min) and the obtained wet pellet (~10 g per liter) were resuspended in lysis buffer (5 ml g^{-1}). The lysis buffer was prepared by ten times dilution of BugBuster 10× (Novagen) using 50 mM phosphate, 300 mM NaCl, 20 mM imidazole at pH 7.6. To the resulting cell-suspension were added 5 mg lysozyme (20 kU mg^{-1}), 1 mg DNase I (deoxyribonuclease I, 650 kU mg^{-1}), 100 μl phenylmethylsulfonyl fluoride (PMSF, 100 mM) with stirring at RT for 1 hr. The resulting lysate was clarified by centrifugation (13,000 × g), and the supernatant purified via immobilized affinity chromatography (Ni-IMAC) at 4°C (AKTA purifier 10) on a HiTrap 5 ml Chelating HP column (Amersham Biosciences). A step-wise gradient of imidazole (25–250 mM) was applied and UV absorbance was monitored at 280 nm. The desired fractions, as detected by sodium dodecyl sulfate polyacrylamide gel (SDS-PAGE) analysis, were pooled. Finally, the homogenous samples were concentrated to 1 ml and washed with PBS (5 × 20 ml) by ultrafiltration (3000 × g at 4°C, in Vivaspin-20, 10,000 MWCO tubes, VivaScience Sartorious group). Protein concentrations were calculated via spectrophotometeric analysis (ε_{280} 79,400 M^{-1} cm^{-1}).

Substrate Screening Assay

Substrate screening was performed in 50 mM potassium phosphate buffer and 145 mM sodium chloride (PBS) (pH 7.6) at 22°C with different *p*NP-glycosides (8 mM) (Figure 2A). Reaction mixtures (180 μl) were preincubated in the cell holder and reactions were initiated by addition of enzyme solutions (20 μl, 0.5 μM WT or mutants). Substrate hydrolysis was determined by monitoring absorbance at 400 nm (ε = 5350 M^{-1} cm^{-1} for *p*-nitrophenolate) using a Molecular Devices SpectraMax Plus^{384} plate reader (Figures 1C and 2A).

Enzyme Hydrolytic Activity Assay

Kinetic studies were performed as described above with different concentrations of *p*NP-β-D-Glc (*para*-nitrophenyl β-D-glucopyranoside) substrate ranging from 1.4 mM to 25 mM. Continuous assays were repeated in triplicate. Kinetic parameters (K_m and V_{max}) were determined by fitting initial velocity data (determined by Softmax Pro V4.6) to the Michaelis–Menten equation by GraFit 5.0 (Erithacus Software).

Synthesis of GlcF and DNP-β-D-Glc

GlcF (Yoon and Rhee, 2000; Juenneman et al., 1991) and DNP-β-D-Glc (Sharma et al., 1995; Ballardie et al., 1973) were synthesized following literature procedures in 85% and 20% yield, respectively.

Preparation of D-Desosamine Hydrochloride

White crystalline D-desosamine-HCl (200 mg) was obtained from acidic hydrolysis of clarithromycin (20 g) according to the similar procedures in the literature (Wiley, 1962; Woo et al., 1962; Bolton et al., 1961; Jaret et al., 1973). No efforts were made to optimize the yield.

Thin Layer Chromatography Analysis

TLC was performed on precoated glass-backed silica gel plates (TLC plate 60A, thickness 250 μm) supplied by Silicycle. Chromatograms were initially

examined under UV light and then visualized with an aqueous potassium permanganate (dip), followed by warming of the TLC plate with a heat gun. Mobile phases for glycosynthase assays were EtOAc/MeOH/Water 5/2/0.5 or n-propanol/NH3/Water 5/1/1. These plates were additionally visualized using vanillin spray or iodine vapor.

Mutant Rescue Experiments

Rescue experiments were performed as described above with different concentrations of external nucleophiles (0.2–4 M sodium formate or 0.25–2 M potassium fluoride). Reaction mixtures (120 μl) were made by preincubation of enzymes (0.5 μM) and external nucleophile in the cell holder followed by addition of DNP-β-D-Glc (80 μl, 1 mM). Substrate hydrolysis was monitored at 400 nm and initial velocity data were corrected by subtracting hydrolysis of substrate in the absence of enzyme.

Glycosynthase Assay

To explore glycosynthase activity of all mutants, 4 mM enzymes were incubated with methymycin (20 mM) and GlcF (80 mM) in PBS (pH 7.6) at 37°C. Reaction mixtures were analyzed by TLC in different intervals up to 2 days and then finally analyzed using HPLC (Dreassi et al., 2000) and mass spectroscopy (ESI^+). Moreover, mutants (0.5 μM) were incubated at RT with GlcF (80 mM) as the donor glycoside and the following acceptors: erythromycin (2.6 mM, saturated solution), *p*NP-β-D-Glc, *p*NP-α-D-Glc, *O*Me-β-D-Gal, methanol, phenol (all at 40 mM concentration).

NMR Experiments

All NMR experiments were performed on a Bruker Avance 500-MHz spectrometer using a 5 mm inverse triple-resonance ($^1H/^{13}C/^{15}N$) probe equipped with a single axis actively shielded Z-gradient coil. STD (saturation transfer difference) spectra (Mayer and Meyer, 1999; Mayer and Meyer, 2001) were typically collected using 32 scans and 4 dummy scans with 32 k total data points covering a sweep width of 18 ppm. Selective saturation of the protein was performed using a 50 ms Gaussian pulse train of 86 Hz field strength. The total saturation time was typically 2 s, unless otherwise specified, and was adjusted by the number of pulses in the saturation train. An additional delay before saturation was applied to keep the total recovery time constant. The saturated and reference spectra were acquired sequentially during each individual scan by creating a pseudo-2D experiment. During each scan, the saturation frequency switched from on-resonance at −1 ppm to off-resonance at −35 ppm. One spectrum was recorded with an on-resonance signal at 8 ppm that resulted in the same STD-NMR pattern (Figure S14). To improve the quality of the STD spectra, a 50 ms, 4960 Hz spin-lock ($T_{1\rho}$filter) was applied to both the on- and off-resonance spectra to eliminate protein background signals, and a 2 ms spoil gradient was incorporated to destroy unwanted magnetization. The spectra were processed using Bruker's TopSpin software, v1.3. The on- and off-resonance spectra were processed identically, using a 2 Hz line broadening function and zero-filling twice before Fourier Transform. STD spectra were obtained by subtracting the saturated spectrum from the reference spectrum. Control STD experiments without protein gave no spectra, indicating that artifacts were negligible. 2D STD-TOCSY spectra were recorded with 16 scans per t1 increment. A total of 64 t1 increments were collected, with the difference between the on and off resonance spectra obtained via the phase cycle. An 80 ms MLEV spin-lock was applied. For STD-NMR experiments, DesR concentrations were typically 0.02 mM, erythromycin concentrations were 2 mM, and spectra were recorded at 300 K. The proton and carbon chemical shifts of erythromycin in d-PBS (pH ~7.6) were assigned by the combined use of 1D- and 2D-NMR spectra including COSY, DQF-COSY, NOESY, ROESY, TOCSY, HSQC, HMBC, DEPTQ-135. Hydrolysis of GlcF was monitored by ^{19}F-NMR spectroscopy according to the literature procedure (Andre et al., 2001; Albert et al., 2000).

Enzymatic Inhibition Assays

An IC_{50} for DesR-WT hydrolysis of *p*NP-β-D-Glc (3.1 mM) was determined by preincubation (2 min) of the enzyme (0.05 μM) in the prescence of various concentrations of erythromycin (5 nM–1 mM), clarithromycin (70 nM–0.2 mM), or azithromycin (0.32 μM–3.2 mM) under conditions described above. K_i values for erythromycin and clarithromycin were determined by measuring the initial velocities at various concentrations of *p*NP-β-D-Glc (1.4–25 mM) with a range of fixed concentrations of inhibitors. Kinetic data using up to 10 μM inhibitors followed Michaelis-Menten curvature and were used for calculation of K_i using Grafit 5.0.

SUPPLEMENTAL DATA

Supplemental data include two schemes, sixteen figures, and three tables and can be found with this article online at http://www.chembiol.com/cgi/content/full/15/7/739/DC1/.

ACKNOWLEDGMENTS

We thank Hung-Wen (Ben) Liu (University of Texas) for pDesR-3 plasmid and methymycin. We thank Stephen Bearne (Dalhousie University) for helpful discussions. This research was supported by Mizutani Foundation of Glycoscience of Japan and the Natural Sciences and Engineering Research Council of Canada.

Received: March 11, 2008
Revised: May 8, 2008
Accepted: May 13, 2008
Published: July 18, 2008

REFERENCES

Albert, M., Repetschnigg, W., Ortner, J., Gomes, J., Paul, B.J., Illaszewicz, C., Weber, H., Steiner, W., and Dax, K. (2000). Simultaneous detection of different glycosidase activities by ^{19}F NMR spectroscopy. Carbohydr. Res. *327*, 395–400.

Andre, C., Spangenberg, P., Gentil, E., and Rabiller, C. (2001). In situ ^{19}F NMR spectroscopy study of enzymatic transglycosylation reactions using α-D-aldohexopyranosyl fluorides as donors and acceptors. Tetrahedron Asymmetry *12*, 779–783.

Armstrong, D.N., Ballantyne, G.H., and Modlin, I.M. (1992). Erythromycin stimulates ileal motility by activation of dihydropyridine-sensitive calcium channels. J. Surg. Res. *52*, 140–146.

Awan, A., Barber, J., Brennan, R.J., and Parkinson, J.A. (1992). Structural studies on clarithromycin (6-O-methylerythromycin A): assignments of the proton and carbon-13 NMR spectra in organic and aqueous solutions. Magn. Reson. Chem. *30*, 1241–1246.

Awan, A., Brennan, R.J., Regan, A.C., and Barber, J. (1995). Conformational analysis of the erythromycin analogs azithromycin and clarithromycin in aqueous solution and bound to bacterial ribosomes. J. Chem. Soc. Chem. Commun. *1995*, 1653–1654.

Ballardie, F., Capon, B., Sutherland, J.D.G., Cocker, D., and Sinnott, M. (1973). Simple general synthesis of 2,4-dinitrophenyl glycopyranosides. J. Chem. Soc., Perkin Trans. 1 *1973*, 2418–2419.

Barber, J., Gyi, J.I., Lian, L., Morris, G.A., Pye, D.A., and Sutherland, J.K. (1991). The structure of erythromycin A in $[^2H_6]$DMSO and buffered D_2O: full assignments of the ^1H and ^{13}C NMR spectra. J. Chem. Soc., Perkin Trans. 2 *1991*, 1489–1494.

Berteau, O., Sandstroem, C., Bielicki, J., Anson, D.S., and Kenne, L. (2003). Glycosidase-substrate interactions analysis by STD-NMR spectroscopy: Study of α-L-fucosidase. J. Am. Chem. Soc. *125*, 15296–15297.

Bolton, C.H., Foster, A.B., Stacey, M., and Webber, J.M. (1961). Carbohydrate components of antibiotics. I. Degradation of desosamine by alkali: its absolute configuration at position 5. J. Chem. Soc. *1961*, 4831–4836.

Brecker, L., Straganz, G.D., Tyl, C.E., Steiner, W., and Nidetzky, B. (2006). Saturation-transfer-difference NMR to characterize substrate binding recognition and catalysis of two broadly specific glycoside hydrolases. J. Mol. Catal., B Enzym. *42*, 85–89.

Burlingham, B.T., and Widlanski, T.S. (2003). An intuitive look at the relationship of Ki and IC50: a more general use of the Dixon plot. J. Chem. Educ. *80*, 214–218.

Coates, A., Hu, Y., Bax, R., and Page, C. (2002). The future challenges facing the development of new antimicrobial drugs. Nat. Rev. Drug Discov. *1*, 895–910.

Culic, O., Erakovic, V., and Parnham, M.J. (2001). Anti-inflammatory effects of macrolide antibiotics. Eur. J. Pharmacol. *429*, 209–229.

Dreassi, E., Corti, P., Bezzini, F., and Furlanetto, S. (2000). High-performance liquid chromatographic assay of erythromycin from biological matrix using electrochemical or ultraviolet detection. Analyst *125*, 1077–1081.

Drone, J., Feng, H.-y., Tellier, C., Hoffmann, L., Tran, V., Rabiller, C., and Dion, M. (2005). Thermus thermophilus glycosynthases for the efficient synthesis of galactosyl and glucosyl β-(1->3)-glycosides. Eur. J. Org. Chem. *2005*, 1977–1983.

Ducros, V.M.A., Tarling, C.A., Zechel, D.L., Brzozowski, A.M., Frandsen, T.P., von Ossowski, I., Schulein, M., Withers, S.G., and Davies, G.J. (2003). Anatomy of glycosynthesis structure and kinetics of the humicola insolens Cel7B E197A and E197S glycosynthase mutants. Chem. Biol. *10*, 619–628.

Dwek, R.A., Butters, T.D., Platt, F.M., and Zitzmann, N. (2002). Targeting glycosylation as a therapeutic approach. Nat. Rev. Drug Discov. *1*, 65–75.

Erbas, T., Varoglu, E., Erbas, B., Tastekin, G., and Akalin, S. (1993). Comparison of metoclopramide and erythromycin in the treatment of diabetic gastroparesis. Diabetes Care *16*, 1511–1514.

Fiese, E.F., and Steffen, S.H. (1990). Comparison of the acid stability of azithromycin and erythromycin A. J. Antimicrob. Chemother. *25*, 39–47.

Fu, X., Albermann, C., Jiang, J., Liao, J., Zhang, C., and Thorson, J.S. (2003). Antibiotic optimization via in vitro glycorandomization. Nat. Biotechnol. *21*, 1467–1469.

Giamarellos-Bourboulis, E.J. (2008). Macrolides beyond the conventional antimicrobials: a class of potent immunomodulators. Int. J. Antimicrob. Agents *31*, 12–20.

Griffith, B.R., Langenhan, J.M., and Thorson, J.S. (2005). 'Sweetening' natural products via glycorandomization. Curr. Opin. Biotechnol. *16*, 622–630.

Hancock, S.M., Vaughan, M.D., and Withers, S.G. (2006). Engineering of glycosidases and glycosyltransferases. Curr. Opin. Chem. Biol. *10*, 509–519.

Haselhorst, T., Wilson, J.C., Liakatos, A., Kiefel, M.J., Dyason, J.C., and von Itzstein, M. (2004). NMR spectroscopic and molecular modeling investigations of the trans-sialidase from Trypanosoma cruzi. Glycobiology *14*, 895–907.

Hawkyard, C.V., and Koerner, R.J. (2007). The use of erythromycin as a gastrointestinal prokinetic agent in adult critical care: benefits versus risks. J. Antimicrob. Chemother. *59*, 347–358.

Henninger, T.C. (2003). Recent progress in the field of macrolide antibiotics. Expert Opin. Ther. Pat. *13*, 787–805.

Hommalai, G., Withers, S.G., Chuenchor, W., Cairns, J.R.K., and Svasti, J. (2007). Enzymatic synthesis of cello-oligosaccharides by rice BGlu1 β-glucosidase glycosynthase mutants. Glycobiology *17*, 744–753.

Honda, Y., and Kitaoka, M. (2006). The first glycosynthase derived from an inverting glycoside hydrolase. J. Biol. Chem. *281*, 1426–1431.

Hrmova, M., and Fincher, G.B. (2001). Structure-function relationships of β-D-glucan endo- and exohydrolases from higher plants. Plant Mol. Biol. *47*, 73–91.

Ianaro, A., Ialenti, A., Maffia, P., Sautebin, L., Rombola, L., Carnuccio, R., Iuvone, T., D'Acquisto, F., and Di Rosa, M. (2000). Anti-inflammatory activity of macrolide antibiotics. J. Pharmacol. Exp. Ther. *292*, 156–163.

Jahn, M., Stoll, D., Warren, R.A.J., Szabo, L., Singh, P., Gilbert, H.J., Ducros, V.M.A., Davies, G.J., and Withers, S.G. (2003). Expansion of the glycosynthase repertoire to produce defined manno-oligosaccharides. Chem. Commun. (Camb). *2003*, 1327–1329.

Jakeman, D.L., and Withers, S.G. (2002). Engineering glycosidases for constructive purposes. In Carbohydrate Bioengineering: Interdisciplinary Approaches, T.T. Teeri, B. Svensson, H.J. Gilbert, and T. Feizi, eds. (Cambridge, UK: Royal Society of Chemistry), pp. 3–8.

Jaret, R.S., Mallams, A.K., and Reimann, H. (1973). Megalomicins. IV. Structures of megalomicins A, B, C1, and C2. J. Chem. Soc., Perkin Trans. *1*, 1374–1388.

Juenneman, J., Lundt, I., and Thiem, J. (1991). Preparation of some 2-deoxy- and 2,6-dideoxy-glycosyl fluorides. Acta Chem. Scand. *45*, 494–498.

Kameda, Y., Asano, N., Takeuchi, M., Yamaguchi, T., Matsui, K., Horii, S., and Fukase, H. (1985). Epivaliolamine and deoxyvalidamine, new pseudo-aminosugars produced by *Streptomyces hygroscopicus*. J. Antibiot. (Tokyo) *38*, 1816–1818.

Lazarevski, G., Vinkovic, M., Kobrehel, G., Dokic, S., Metelko, B., and Vikic-Topic, D. (1993). Conformational analysis of azithromycin by NMR spectroscopy and molecular modeling. Tetrahedron *49*, 721–730.

Maxwell, V.L., Evinson, E.L., Emmerson, D.P.G., and Jenkins, P.R. (2006). Synthesis, glycosidase activity and X-ray crystallography of 3-amino-sugars. Org. Biomol. Chem. *4*, 2724–2732.

Mayer, M., and Meyer, B. (1999). Characterization of ligand binding by saturation transfer difference NMR spectroscopy. Angew. Chem. Int. Ed. Engl. *38*, 1784–1788.

Mayer, M., and Meyer, B. (2001). Group epitope mapping by saturation transfer difference NMR to identify segments of a ligand in direct contact with a protein receptor. J. Am. Chem. Soc. *123*, 6108–6117.

Mendez, C., and Salas, J.A. (2001). Altering the glycosylation pattern of bioactive compounds. Trends Biotechnol. *19*, 449–456.

Omura, S., Tsuzuki, K., Sunazuka, T., Toyota, H., Takahashi, I., and Itoh, Z. (1985). Gastrointestinal motor-stimulating activity of macrolide antibiotics and the structure-activity relationship. J. Antibiot. (Tokyo) *38*, 1631–1632.

Pyetan, E., Baram, D., Auerbach-Nevo, T., and Yonath, A. (2007). Chemical parameters influencing fine-tuning in the binding of macrolide antibiotics to the ribosomal tunnel. Pure Appl. Chem. *79*, 955–968.

Quiros, L.M., Hernandez, C., and Salas, J.A. (1994). Purification and characterization of an extracellular enzyme from Streptomyces antibioticus that converts inactive glycosylated oleandomycin into the active antibiotic. Eur. J. Biochem. *222*, 129–135.

Rao, F.V., Houston, D.R., Boot, R.G., Aerts, J.M.F.G., Hodkinson, M., Adams, D.J., Shiomi, K., Omura, S., and van Aalten, D.M.F. (2005). Specificity and affinity of natural product cyclopentapeptide inhibitors against *A. fumigatus*, human, and bacterial chitinases. Chem. Biol. *12*, 65–76.

Rubin, B. (2004). Immunomodulatory properties of macrolides: overview and historical perspective. Am. J. Med. *117*, S2–S4.

Salleh, H.M., Mullegger, J., Reid, S.P., Chan, W.Y., Hwang, J., Warren, R.A., and Withers, S.G. (2006). Cloning and characterization of *Thermotoga maritima* β-glucuronidase. Carbohydr. Res. *341*, 49–59.

San Jose, E., Munoz-Fernandez, M.A., and Alarcon, B. (1997). Megalomicin inhibits HIV-1 replication and interferes with gp160 processing. Virology *239*, 303–314.

Schlunzen, F., Zarivach, R., Harms, J., Bashan, A., Tocilj, A., Albrecht, R., Yonath, A., and Franceschl, F. (2001). Structural basis for the interaction of antibiotics with the peptidyl transferase center in eubacteria. Nature *413*, 814–821.

Sharma, S.K., Corrales, G., and Penades, S. (1995). Single step stereoselective synthesis of unprotected 2,4-dinitrophenyl glycosides. Tetrahedron Lett. *36*, 5627–5630.

Shiono, T., and Hayasaka, S. (1985). Aminoglycoside antibiotics and lysosomal enzymes of human tears. Arch. Ophthalmol. *103*, 1747–1749.

Sweetman, S.C. (2002). Martindale. The Complete Drug Reference, 33rd Edition (London: Pharmaceutical Press).

Takeuchi, M., Kamata, K., Yoshida, M., Kameda, Y., and Matsui, K. (1990). Inhibitory effect of pseudo-aminosugars on oligosaccharide glucosidases I and II and on lysosomal α-glucosidase from rat liver. J. Biochem. (Tokyo) *108*, 42–46.

Thibodeaux, C.J., and Liu, H.-W. (2007). Manipulating nature's sugar biosynthetic machineries for glycodiversification of macrolides: recent advances and future prospects. Pure Appl. Chem. *79*, 785–799.

Thibodeaux, C.J., Melancon, C.E., and Liu, H.-W. (2007). Unusual sugar biosynthesis and natural product glycodiversification. Nature *446*, 1008–1016.

Thiem, J. (1995). Applications of enzymes in synthetic carbohydrate chemistry. FEMS Microbiol. Rev. *16*, 193–211.

Vaughan, M.D., Johnson, K., DeFrees, S., Tang, X., Warren, R.A.J., and Withers, S.G. (2006). Glycosynthase-mediated synthesis of glycosphingolipids. J. Am. Chem. Soc. *128*, 6300–6301.

Walsh, C., Freel Meyers, C.L., and Losey, H.C. (2003). Antibiotic glycosyltransferases: antibiotic maturation and prospects for reprogramming. J. Med. Chem. *46*, 3425–3436.

Wang, Q., Graham, R.W., Trimbur, D., Warren, R.A.J., and Withers, S.G. (1994). Changing enzymic reaction mechanisms by mutagenesis: Conversion of a retaining glucosidase to an inverting enzyme. J. Am. Chem. Soc. *116*, 11594–11595.

Wang, L., Kitaichi, K., Hui, C.S., Takagi, K., Takagi, K., Sakai, M., Yokogawa, K., Miyamoto, K.-I., and Hasegawa, T. (2000). Reversal of anticancer drug resistance by macrolide antibiotics in vitro and in vivo. Clin. Exp. Pharmacol. Physiol. *27*, 587–593.

Wang, Y.-S., Liu, D., and Wyss, D.F. (2004). Competition STD NMR for the detection of high-affinity ligands and NMR-based screening. Magn. Reson. Chem. *42*, 485–489.

Wen, X., Yuan, Y., Kuntz, D.A., Rose, D.R., and Pinto, B.M. (2005). A combined STD-NMR/molecular modeling protocol for predicting the binding modes of the glycosidase inhibitors kifunensine and salacinol to golgi α-mannosidase II. Biochemistry *44*, 6729–6737.

White, A.A., and Simon, R.A. (2005). Macrolide antibiotics as anti-inflammatory agents. Curr. Allergy Asthma Rep. *5*, 1–3.

Wiley, P.F. (1962). Desosamine hydrochloride. From erythromycin. In Methods in Carbohydrate Chemistry, M.L. Wolfrom, J.N. BeMiller, and R.L. Whistler, eds. (New York: Academic Press), pp. 257–259.

Williams, S.J., Mark, B.L., Vocadlo, D.J., James, M.N.G., and Withers, S.G. (2002). Aspartate 313 in the Streptomyces plicatus hexosaminidase plays a critical role in substrate-assisted catalysis by orienting the 2-acetamido group and stabilizing the transition state. J. Biol. Chem. *277*, 40055–40065.

Winchester, B., and Fleet, G.W.J. (1992). Amino-sugar glycosidase inhibitors: versatile tools for glycobiologists. Glycobiology *2*, 199–210.

Woo, P.W.K., Dion, H.W., Durham, L., and Mosher, H.S. (1962). Stereochemistry of desosamine. An N.M.R. analysis. Tetrahedron Lett. *1962*, 735–739.

Yan, J., Kline, A.D., Mo, H., Shapiro, M.J., and Zartler, E.R. (2003). The effect of relaxation on the epitope mapping by saturation transfer difference NMR. J. Magn. Reson. *163*, 270–276.

Yang, J., Hoffmeister, D., Liu, L., Fu, X., and Thorson, J.S. (2004). Natural product glycorandomization. Bioorg. Med. Chem. *12*, 1577–1584.

Yang, M., Davies, G.J., and Davies, B.G. (2007). A glycosynthase catalyst for the synthesis of flavonoid glycosides. Angew. Chem. Int. Ed. Engl. *46*, 3885–3888.

Yatsunami, J., Fukuno, Y., Nagata, M., Tominaga, M., Aoki, S., Tsuruta, N., Kawashima, M., Taniguchi, S.I., and Hayashi, S.-I. (1999). Antiangiogenic and antitumor effects of 14-membered ring macrolides on mouse B16 melanoma cells. Clin. Exp. Metastasis *17*, 361–367.

Yoon, J.H., and Rhee, J.S. (2000). The efficient enzymatic synthesis of N-acetyllactosamine in an organic co-solvent. Carbohydr. Res. *327*, 377–383.

Zalewska-Kaszubska, J., and Gorska, D. (2001). Anti-inflammatory capabilities of macrolides. Pharmacol. Res. *44*, 451–454.

Zhang, C., Fu, Q., Albermann, C., Li, L., and Thorson Jon, S. (2007). The in vitro characterization of the erythronolide mycarosyltransferase EryBV and its utility in macrolide diversification. ChemBioChem *8*, 385–390.

Zhao, L., Sherman, D.H., and Liu, H.-W. (1998). Biosynthesis of desosamine: Molecular evidence suggesting β-glucosylation as a self-resistance mechanism in methymycin/neomethymycin producing strain, *Streptomyces venezuelae*. J. Am. Chem. Soc. *120*, 9374–9375.

Zhao, L., Beyer, N.J., Borisova, S.A., and Liu, H.-W. (2003). β-Glucosylation as a part of self-resistance mechanism in mthymycin/pikromycin producing strain *Streptomyces venezuelae*. Biochemistry *42*, 14794–14804.

Note Added in Proof

A recent pH screening method for glycosynthases has recently been published that may be applicable to the DesR system:

Ben-David, A., Shoham, G., and Shoham, Y. (2008). A universal screening assay for glycosynthases: directed evolution of glycosynthase XynB2(E335G) suggests a general path to enhance activity. Chem. Biol. *15*, 546–551.